Hemispheric ozone variability indices derived from satellite observations and comparison to a coupled chemistry-climate model

T. Erbertseder, V. Eyring, M. Bittner, M. Dameris, V. Grewe

Atmos. Chem. Phys., 6, 5105–5120, 2006
www.atmos-chem-phys.net/6/5105/2006/

Atmospheric Chemistry and Physics

Hemispheric ozone variability indices derived from satellite observations and comparison to a coupled chemistry-climate model

T. Erbertseder[1], **V. Eyring**[2], **M. Bittner**[1], **M. Dameris**[2], **and V. Grewe**[2]

[1]German Remote Sensing Data Center, DFD, German Aerospace Center, DLR, Wessling, Germany
[2]Institute for Atmospheric Physics, German Aerospace Center, DLR, Wessling, Germany

Received: 4 April 2006 – Published in Atmos. Chem. Phys. Discuss.: 30 June 2006
Revised: 19 October 2006 – Accepted: 3 November 2006 – Published: 7 November 2006

Abstract. Total column ozone is used to trace the dynamics of the lower and middle stratosphere which is governed by planetary waves. In order to analyse the planetary wave activity a Harmonic Analysis is applied to global multi-year total ozone observations from the Total Ozone Monitoring Spectrometer (TOMS). As diagnostic variables we introduce the hemispheric ozone variability indices one and two. They are defined as the hemispheric means of the amplitudes of the zonal waves number one and two, respectively, as traced by the total ozone field.

The application of these indices as a simple diagnostic for the evaluation of coupled chemistry-climate models (CCMs) is demonstrated by comparing results of the CCM ECHAM4.L39(DLR)/CHEM (hereafter: E39/C) against satellite observations. It is quantified to what extent a multi-year model simulation of E39/C (representing "2000" climate conditions) is able to reproduce the zonal and hemispheric planetary wave activity derived from TOMS data (1996–2004, Version 8).

Compared to the reference observations the hemispheric ozone variability indices one and two of E39/C are too high in the Northern Hemisphere and too low in the Southern Hemisphere. In the Northern Hemisphere, where the agreement is generally better, E39/C produces too strong a planetary wave one activity in winter and spring and too high an interannual variability. For the Southern Hemisphere we reveal that the indices from observations and model differ significantly during the ozone hole season. The indices are used to give reasons for the late formation of the Antarctic ozone hole, the insufficient vortex elongation and eventually the delayed final warming in E39/C.

In general, the hemispheric ozone variability indices can be regarded as a simple and robust diagnostic to quantify model-observation differences concerning planetary wave activity. It allows a first-guess on how the dynamics is represented in a model simulation before applying costly and more specific diagnostics.

Correspondence to: T. Erbertseder
(thilo.erbertseder@dlr.de)

1 Introduction

Quantifying the distribution and variability of ozone over a wide range of scales, both temporal and spatial, has been an intense subject of scientific research. With the advent of satellite-borne instruments in the 1970s, global observations of total column ozone have been performed on a routine basis. Observations of the Total Ozone Monitoring Spectrometer (TOMS) since November 1978 have been enabled to study the morphology, depth and evolution of the Antarctic ozone hole (Stolarski et al., 1986; Newman et al., 1986; Schoeberl et al., 1986) and the occurrence and size of low ozone events at mid-latitudes (James, 1998; Bojkov and Balis, 2001). Together with other satellite-borne instruments (BUV and SBUV (Solar Backscatter UV), TOVS and ATOVS (Advanced TIROS Operational Vertical Sounder), GOME (Global Ozone Monitoring Experiment), SCIAMACHY (Scanning Imaging Absorption Spectrometer for Atmospheric Cartography), OMI (Ozone Monitoring Instrument)) and the ground-based network, a continuous global monitoring of total column ozone and its trends with special attention to high and mid-latitudes is possible. Today there is broad agreement that in order to detect signs of ozone recovery (e.g. Newchurch et al., 2003; Steinbrecht et al., 2004; Yang et al., 2005; Huck et al., 2005; Hadjinicolaou et al., 2005; Dameris et al., 2005, 2006) a continuous monitoring of the ozone layer as well as a good understanding of the underlying processes that govern ozone variability is needed (IPCC, 2001; WMO, 2003, chapters 3 and 4).

Published by Copernicus GmbH on behalf of the European Geosciences Union.

Considerable work has been performed to study relationships between total ozone column and atmospheric dynamics and chemistry. For example, studies to correlate the ozone total column ozone with weather systems were made as early as by Dobson (1926) and by Reed (1950). Ozone variability exhibits signals due to a large variety of processes induced by the 11-year solar cycle (e.g. Haigh, 1996; Zerefos et al., 1997; Labitzke et al., 2002), the Quasi Biennial Oscillation (e.g. Bojkov and Fioletov, 1995; Zerefos et al., 1992), the El Nino Southern Oscillation (e.g. Kayano, 1997), North Atlantic Oscillation (e.g. Schnadt and Dameris, 2003; Appenzeller et al., 2000) and Arctic Oscillation (e.g. Nikulin and Repinskaya, 2001). The significant influence of chemistry on ozone is indicated by trends related to the increase of anthropogenic emissions like stratospheric halogen compounds since the 1970s (WMO, 2003, chapters 3 and 4) and by episodic volcanic eruptions (e.g. Robock, 2000). Another part of the observed ozone variability can be attributed to meteorological conditions and phenomena like jet streams (e.g. Shapiro, 1981), anticyclones and blocking high pressure systems (Dameris et al., 1995), cyclogenesis and cut-off lows (Thomas et al., 2003). The impact of these factors on the total ozone variations was recently quantified by Steinbrecht et al. (2003) by a multi-linear regression analysis using TOMS data.

It has been shown that total column ozone can be considered as a tracer for stratospheric dynamics. Especially, planetary waves were found to explain the total ozone variability (Wirth, 1993). This is because the chemical lifetime of ozone in the lower and middle stratosphere, where approximately 90% of the vertical ozone abundance is found, is long enough that it may be considered as tracer for transport processes. In turn, total ozone is an excellent tracer to quantify wave-induced variability of the stratosphere. The focus of this work is on planetary-scale waves following these findings of Wirth (1993).

Planetary-scale waves are frequently observed in the middle atmosphere (stratosphere and mesosphere). In their simplest form of Rossby-waves they occur due to the variation of the Coriolis parameter with latitude (e.g. Andrews et al., 1987). They show up as transient waves with periods of several days to a few weeks while excitation and decay occurs on time scales of 1–2 months (Salby, 1984). Some of these large-scale waves are forced by features at the surface, by orography and thermal contrast, e.g. between land and sea. In that case they are (quasi-) stationary with respect to the surface. There are several reasons that motivate the substantial interest in these phenomena. Planetary waves drive the circulation away from radiative equilibrium. They are known to be an important source mechanism for transport processes in the stratosphere, are responsible for the intermittent midwinter breakdown of the polar vortices called sudden stratospheric warmings and are involved in vortex erosion processes (e.g. Schoeberl and Hartmann, 1991).

The activity of planetary waves can be characterized by their amplitude. Based on total column ozone as a tracer, the amplitude of the quasi-stationary waves can be derived from satellite observations on a daily basis (Bittner et al., 1997). Thus, total ozone can be used as a proxy to quantify planetary wave activity. In order to derive the activity of the planetary waves number one and two we apply a Harmonic Analysis to total ozone observations from the Total Ozone Monitoring Spectrometer (TOMS) from 1978 to 2004. The TOMS data provides a consistent record with proven accuracy and well suited temporal and spatial resolution. Based on this approach and data we derive time series of hemispheric ozone variability indices, simple quantities to reveal and represent the integrated hemispheric planetary wave activity.

While satellite and ground-based instruments allow ozone variation to be observed, coupled chemistry-climate models (CCMs) with detailed descriptions of the stratosphere can address how climate change, stratospheric ozone and UV radiation interact, now and in the future (Austin et al., 2003; Eyring et al., 2006). Therefore, these models provide fundamental information for ozone, UV and climate assessments (SPARC, 1998; WMO, 2003, chapters 3 and 4; IPCC/TEAP, 2005, chapter 1).

In order to gain reliable results CCMs have to realistically represent chemical and dynamical processes like forcing and propagation of planetary-scale waves (Eyring et al., 2005). We therefore introduce the hemispheric ozone variability indices as diagnostic to examine the ability of a CCM to describe planetary wave activity. We exemplify this general diagnostic by comparing indices based on TOMS as reference with indices based on E39/C. We introduce the application, discuss the temporal and spatial variability and point out the differences of the diagnostic variables.

The presented diagnostic is based on a simple quantity derived from observed total ozone data that acts as a tracer for planetary wave activity. Contrary to reanalysed meteorological data it is not influenced by model biases. Additionally, TOMS total ozone data is very well validated and is freely and easily available. The diagnostic is intended as a supplement that gives a first-guess on how the dynamics is represented in a model simulation before applying costly and specific diagnostics. Finally, we would like to emphasise the straightforwardness of the diagnostics and its suitability for multi-model comparisons.

The paper is structured as follows: Sect. 2 gives an overview on the satellite observations and the model simulation used in this analysis. The spectral statistical approach that has been developed to derive zonal amplitudes from total ozone fields is described in Sect. 3. Section 4 summarizes results on total ozone variability and hemispheric ozone variability indices. We end with a conclusion.

Table 1. Driving Parameters for the E39/C time-slice experiment under "2000" conditions.

		2000	Reference
CO_2	[ppmv]	376	IPCC (2001)
CH_4	[ppmv]	1.76	IPCC (2001)
N_2O	[ppbv]	316	IPCC (2001)
Cl_y	[ppbv]	3.4	WMO (1999)
NO_x lightning	(Tg(N)/year)	5.0	Grewe et al. (2001)
NO_x air traffic	(Tg(N)/year)	0.7	Schmidt and Brunner (1997)
NO_x surface (industry, traffic)	(Tg(N)/year)	33.0	Benkovitz et al. (1996)
NO_x surface (soils)	(Tg(N)/year)	5.6	Yienger and Levy (1995)
NO_x surface (biomass burning)	(Tg(N)/year)	7.0	Hao et al. (1990)

2 Data

2.1 Satellite observations

To analyse the zonal and hemispheric ozone variability and the ability of the CCM to reproduce this variability we consider backscatter measurements of the Total Ozone Monitoring Spectrometer (TOMS) which has been operated on different platforms since 1978 (McPeters et al., 1998).

TOMS samples backscattered ultraviolet radiation at six wavelengths and provides a continuous mapping of total column ozone. It provides almost complete daily global coverage of ozone outside the polar night region. We apply TOMS data in the most recent version 8.0 (Bhartia and Wellemeyer, 2004), thus TOMS on METEOR-3 is not used.

TOMS V8 uses only two wavelengths (317.5 and 331.2 nm) to derive total ozone while the other 4 wavelengths (depending on the instrument version) are used for diagnostics and error corrections. The algorithm improvements include an aerosol/glint correction based on the aerosol index, new climatologies for ozone profiles, temperature profiles and tropospheric ozone, an improved surface reflectivity model and a more accurate radiative transfer calculation in the forward model. The algorithm is capable of producing total ozone with a root-mean-square precision of about 2%. The errors, however, typically increase with solar zenith angle and in the presence of heavy aerosol loading (Bhartia and Wellemayer, 2004).

TOMS observations give an excellent and representative data record to study the zonal ozone variability and to evaluate model results. Since the focus of the study is neither on absolute values nor on trends, the results are not influenced by any instrument degradation.

2.2 Model description and design of model simulations

ECHAM4.L39(DLR)/CHEM (hereafter: E39/C) is a coupled chemistry-climate model (CCM) which has been used for different studies regarding past and future atmospheric composition and has been compared to observations (Hein et al., 2001; Schnadt et al., 2002; Eyring et al., 2003; Dameris et al., 2005; Steinbrecht et al., 2006). The model has been participating in detailed assessments of CCMs of the stratosphere (Austin et al., 2003; Eyring et al., 2006). For this study, a horizontal resolution of T30 and a corresponding Gaussian transform latitude-longitude grid of $3.75° \times 3.75°$ is employed, on which model physics, chemistry, and tracer transport are calculated. In the vertical the model has 39 layers extending from the surface to the top centred at 10 hPa (Land et al., 2002). The chemistry model CHEM (Steil et al., 1998) is based on the family concept. It includes the most important gaseous and heterogeneous reactions to simulate upper tropospheric and lower stratospheric ozone chemistry.

A time-slice experiment, which in contrast to a transient model simulation is performed with fixed boundary conditions for a specific year, has been carried out under "2000" conditions for this study. In addition to the E39/C version used in Schnadt et al. (2002), photolysis at solar zenith angles higher than 87.5° is included (Lamago et al., 2003) with chemical kinetics based on Sander et al. (2000). A detailed description of the updated model version is given in Dameris et al. (2005).

Mixing ratios for well-mixed greenhouse gases (CO_2, N_2O, CH_4) for the 2000 time-slice simulation are prescribed according to observations (IPCC, 2001). The upper boundary values for Cl_x, NO_y, and zonal chlorofluorocarbon (CFC) fields are taken from a transient model simulation of the Mainz 2-D model, adapted to observations (WMO, 1999). Anthropogenic as well as natural emissions of nitrogen oxides (NO_x=NO+NO_2) are also considered. Table 1 summarizes mixing ratios of greenhouse gases and different NO_x emissions from anthropogenic and natural sources. Sea surface temperatures (SSTs) are prescribed as monthly mean values following the global sea ice and sea surface temperature (HadISST1) data set provided by the UK Met Office Hadley Centre (Rayner et al., 2003). The data are averaged over the years 1995 to 1998.

3 Method

3.1 Harmonic analysis

In order to quantify the zonal variability in total ozone we apply a spectral statistical Harmonic Analysis approach to monthly means of TOMS total ozone observations and vertically integrated ozone fields of E39/C. To allow a later comparison to the model results, the satellite observations were regridded to the spatial discretisation T30 of E39/C which equals a longitude-latitude grid of $3.75° \times 3.75°$.

The applied analysis technique was developed on the basis of Bittner et al. (1994) and makes use of the concept of the deconvolution of the power spectrum at selected latitudes to produce amplitudes and phases for individual longitudinal sinusoidals. A power spectrum is calculated and the dominant spectral feature (phase and amplitude) is determined. A sinusoid to that spectral feature is fitted to the data (Eq. 1) by means of least squares (Eq. 2). The residuals are computed and a second trigonometric function is fitted to the residuals. This procedure is repeated for all harmonics (eight in this case). Additionally, at each step all previous determined spectral components are fitted again, iteratively. This is because the resulting linear combination of sinusoids turns out not to be unimodal when fitting the data. In other words, the variance of the data series can be reduced if the current and the former sinusoidals are varied simultaneously. Bittner et al. (1994) have shown that this "all step mode" allows one to find a much better parameter vector for the least squares scheme than a "one step mode" like the Fourier Analysis. The sinoid can be denoted as

$$\hat{y}_{ik} = \sum_{j=1}^{n} A_{ij} \sin\left(\omega_{ij}\lambda_{ik} - \varphi_{ij}\right), \tag{1}$$

where $\hat{y}_{ik}$ represents the k-th total column ozone value as derived from TOMS or E39/C within the i-th latitude segment, n denotes the number of sinusoidals used, A_{ij} is the amplitude of the j-th oscillation within the i-th latitude segment, and ω_{ij} denotes the angular frequency of the j-th oscillation. λ_{ik} stands for the longitude at the k-th measurement value in the i-th latitude segment and φ_{ij} represents the phase of the i-th oscillation for latitude segment i.

The best fit is determined by the condition

$$\sum_{i=1}^{m}\sum_{j=1}^{n}\left(\hat{y}_{ij} - y_{ij}\right)^2 \quad \Rightarrow \quad \min. \tag{2}$$

The Harmonic Analysis approach accounts for about 98% of the variance of the data when superimposing eight harmonics. However, since in this case 24 free parameters have to be estimated by a set of nonlinear equations, converging problem have to be overcome. Therefore, the Newton-Raphson solver for nonlinear systems of equations is applied (Ortega and Rheinboldt, 1970).

For physical reasons some constraints are evident. The fitted zonal sinusoidal functions are well suited, as mentioned before, to describe the global circulation pattern of the lower and middle stratosphere by modelling the zonal structure of such waves (e.g. Barnett and Labitzke, 1990). This point, however, defines a constraint for the Harmonic Analysis of total ozone data because planetary waves are global phenomena, which means that the wavelengths must be the same at all latitudes while amplitudes and phases are allowed to vary.

However, the Harmonic Analysis shows significant improvements compared to a Fourier-Analysis, which can cause leakage and anti-aliasing effects and is, mathematically speaking, strictly defined for infinite data series only.

3.2 Hemispheric ozone variability indices

Total column ozone fields are utilised to trace the variability due to dynamical processes in the stratosphere. Following Wirth (1993) the total ozone variability on a monthly mean basis can mostly be explained by planetary wave number one and two. In order to quantify the zonal total ozone variability, the amplitudes of the zonal wave number one and two are derived as a function of latitude.

As diagnostic variables we introduce hemispheric ozone variability indices number one and two. They are defined as the hemispheric mean amplitudes of the zonal waves number one and two, respectively, as traced by the total ozone field and derived by the Harmonic Analysis (Sect. 3.1). If the analysis is confined to wave numbers one and two in the total ozone field it will result in true climatological (mean) features, while for wave number three and higher the interannual variation is of the same order than the average.

Notwithstanding the fact that the zonal waves in total column ozone can be interpreted as a manifestation of the quasi-stationary planetary waves, there is a small contribution of chemical processes, but which is negligible on the time scales considered here. Hence, this does not affect the main subject of this study.

Since the indices give an integrated hemispheric measure of planetary wave activity, they are derived from multi-year TOMS total ozone observations first. In a second step we present the application of these indices for evaluating model results of CCMs in general. This application of the indices as diagnostics is exemplified by results of E39/C.

4 Results

4.1 TOMS

4.1.1 Time series of hemispheric ozone variability index 1 (1978 to 2004)

Figure 1 shows time series of the monthly mean hemispheric ozone variability index one for the Northern (top) and Southern Hemisphere (bottom). It is derived from all TOMS ob-

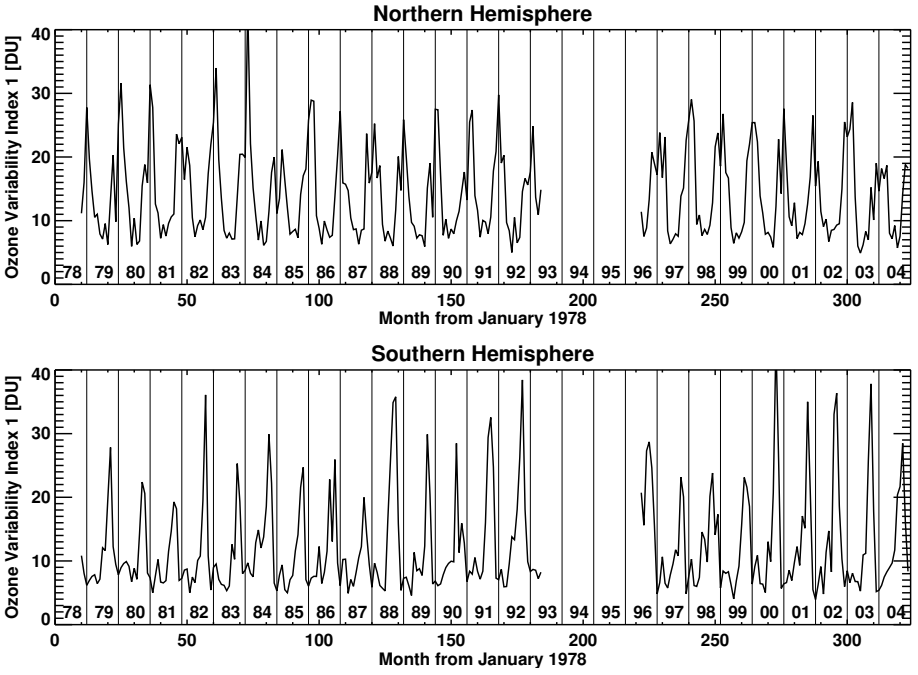

Fig. 1. Time series of the monthly mean hemispheric ozone variability index 1 derived from TOMS total ozone observations from 1978 to 2004 for the Northern (top) and Southern Hemisphere (bottom). Only TOMS data of version 8.0 is used. Thus, TOMS on METEOR is not considered.

servations (V 8.0) from November 1978 to April 1993 and from July 1996 to December 2004. The dominant feature of the time series is a pronounced annual cycle. Yearly maxima from 20 to 40 Dobson Units are found during winter, minima of 5 to 8 DU occur during summer. Note, that there is a clear anticorrelation in wave activity between the hemispheres. This is interpreted as a lack of planetary wave activity during the summer months, when the mean stratospheric flow is easterly and therefore prevents planetary waves from vertical propagation into the stratosphere. This is consistent with the findings first obtained by Charney and Drazin (1961). Enhanced wave one activity, however, can be identified in the Northern Hemisphere, at least occasionally during summer months. These signatures cannot be explained with the abovementioned theory of planetary waves propagating from the troposphere into the lower stratosphere. In the Southern Hemisphere the largest indices are found during austral spring. This is associated to an off-pole displacement of the polar vortex and reflects partly increased amplitudes in the zonal ozone field due to reduced ozone levels inside the vortex.

4.1.2 Interannual variability of hemispheric ozone variability index 1 and 2 (1978 to 2004)

The interannual mean and standard deviation of the hemispheric ozone variability indices one and two for both hemispheres and each month is shown in Fig. 2. Again, the results are derived for all available TOMS total ozone observations (Version 8) between November 1978 and October 2004. Both indices show a characteristic annual cycle for each hemisphere. In the Northern Hemisphere the observed maximum of 24 DU can be found in February, the minimum of 7 DU in June. This reflects the peaking dynamic activity in late winter and the discontinued upward propagation of tropospheric waves in summer. Consequently, the standard deviation of the index for the Northern Hemisphere is highest in February and lowest from June to September.

In the Southern Hemisphere the minimum can be found in January (7 DU) and the maximum in October (27 DU). Compared to a more sinusoidal annual cycle in the Northern Hemisphere, we observe a sharp decrease from October to low values in December, which can be associated with the breakdown of the polar vortex. The annual cycle of the standard deviation is very similar to that of the Northern Hemisphere considering the season. However, high interannual variability is extended into spring and shows a maximum during October. The maxima in October of both, mean and standard deviation, results from the off-pole displacement of the polar vortex leading to large zonal amplitudes of wave number one in the ozone field, and will be discussed later.

The annual cycles of the hemispheric ozone variability index two follows the behaviour of index one to some extent. In the Northern Hemisphere, the maximum of 12 DU is found in February, the yearly minimum of 5 DU occurs in August. The interannual variability is highest in winter

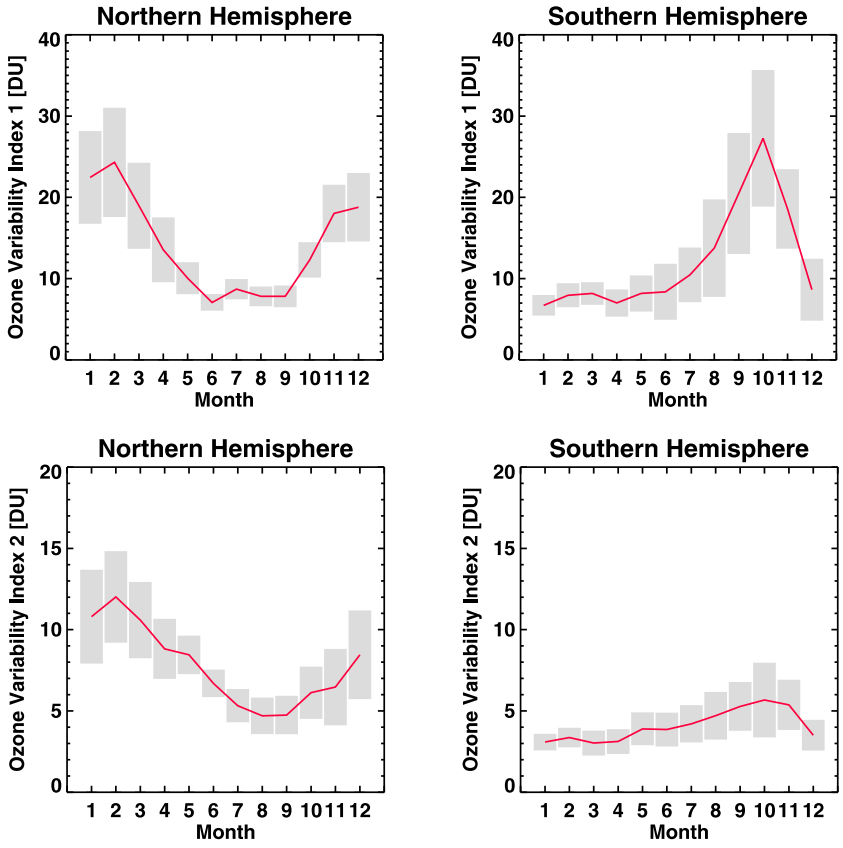

Fig. 2. Interannual mean and standard deviation of the hemispheric ozone variability index 1 (top) and 2 (bottom) for each month (Northern Hemisphere left; Southern Hemisphere right). The results are derived for all available TOMS total ozone observations (Version 8) between November 1978 and October 2004. Note the different scale of the y-axis for indices one and two. The grey bars indicate the standard deviation.

including March. In the Southern Hemisphere index two shows a relatively smooth behaviour. Both mean and standard deviation are lowest from January to April and increase peaking in October. This behaviour agrees with the hemispheric variability index one. The largest standard deviation in October mirrors the elongation of the polar vortex.

4.2 Comparison of TOMS and E39/C

In order to demonstrate the capability of the introduced indices as diagnostic we apply them to compare satellite observations with results of a time slice experiment of E39/C. The time slice experiment results comprise 20 years representative of the atmospheric conditions in the year 2000 (hereafter: E2000). Since the "years" of the time slice experiment do not represent the same chronological order as in the atmosphere as observed by TOMS, no single year can be compared directly. Instead, the experiment has the advantage of giving different realisations of the same year and thus, the focus of this study is on interannual means and variability. In order to provide adequate atmospheric observations for the year 2000 simulation, TOMS data between November 1996 and October 2004 (hereafter: T2000) are considered. These eight years sufficiently reflect perturbed stratospheric chemistry and polar vortex dynamics around the year 2000.

Although T2000 consists of 8 years only, which is a short period on climatological time scales, it can be shown that this period gives a mean representation of the ozone variability on a hemispheric scale. Not only for the Southern, but also for the Northern Hemisphere the hemispheric indices are comparable when two different periods are considered (1978 to 2004 in Fig. 2 and 1996 to 2004 in Figs. 7 and 8). The hemispheric indices are thus robust parameters that reflect the mean hemispheric state and standard deviation. As can be inferred from Fig. 1 it is not sensitive to outliers like the polar vortex split in September 2002.

4.2.1 Total ozone zonal means

Since the diagnostic is based on total ozone we start by discussing zonal means of total ozone and their variability. Figure 3 (top) shows a comparison of total ozone zonal means and standard deviations for T2000 and E2000. Results are presented for the selected months January, April,

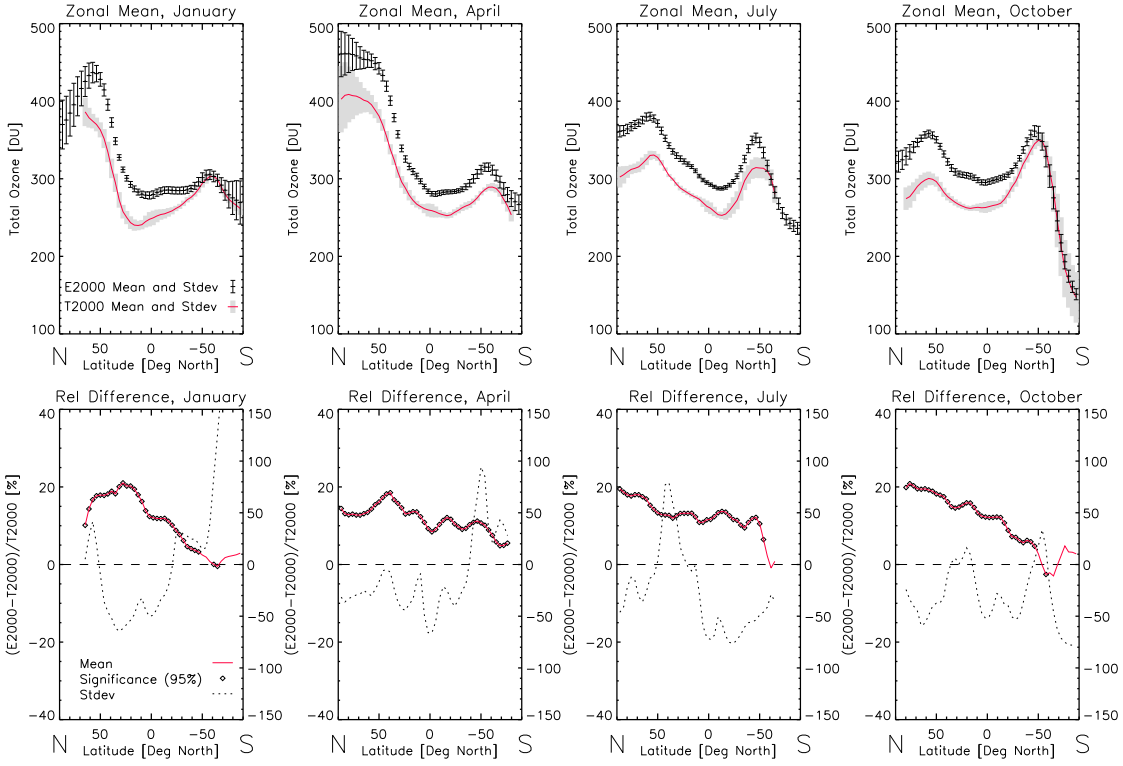

Fig. 3. Zonal means of total ozone for January, April, July and October (top). 20 years of the E39/C time slice experiment "2000" (E2000) are compared to corresponding TOMS data (T2000). E2000 is represented by bars in black (mean and standard deviation), T2000 by the solid (red) curve and grey bars (mean and standard deviation). Below the corresponding relative differences of the means (left y-axis) and the standard deviations (right y-axis) are denoted. A diamond indicates statistically significant differences of the population means at the 5% level (i.e. confidence level of 95%).

July and October. These months are chosen to represent typical seasonal conditions, which gives a clearer picture than seasonal means. The corresponding relative differences for mean and standard deviation (Fig. 3, bottom) also depict the statistical significance.

The zonal means of T2000 show the well known features and seasonal variability of total ozone. While the amounts are nearly constant in the tropics (around 240 to 260 DU), recognizable also by the low standard deviations, high levels occur at northern mid and high latitudes in winter and spring (January and April). The massive depletion of stratospheric ozone in austral spring results in strongly reduced ozone columns in October at southern polar latitudes. Here a total column reduction below 220 DU indicates ozone hole conditions.

When comparing T2000 and E2000 zonal means of total ozone throughout all seasons a good latitudinal agreement of the shape of the statistical moments can be found. Worth mentioning is the latitudinal agreement of the mid-latitude ozone maximum in both hemispheres. As the only exception the ozone maximum between 50° S to 60° is shifted equatorwards in E39/C (up to 10° in April). This can be attributed to an equatorward displacement of the summer vortex, which was also identified in the zonal winds of a transient run of E39/C (Dameris et al., 2005).

Contrary to the structural agreement a positive bias of E39/C is evident in all months with maxima up to 20% north of 20° N (Fig. 3, bottom). The largest absolute positive bias is found north of 40° N with 60 DU. The bias is smallest in southern polar latitudes (<50° S). There is no significant difference in the total ozone zonal means south of 50° S in January, July and October. Notably, the Antarctic ozone hole levels are well met.

Figure 3 further reveals that E2000 generally underestimates the standard deviation, which stands for the zonal variability. Positive exceptions are associated with the north hemispheric mid-latitude ozone maximum in July and latitudes south of 40° S in January and April. The highest positive bias in the standard deviation occurs in southern polar latitudes in January. This is related to the persistent polar vortex in E39/C and will be resumed later in more detail.

When analysing zonal means of total ozone, it has to be stressed that 8 years are too short a period to quantify a significant climatological zonal mean state, especially for the

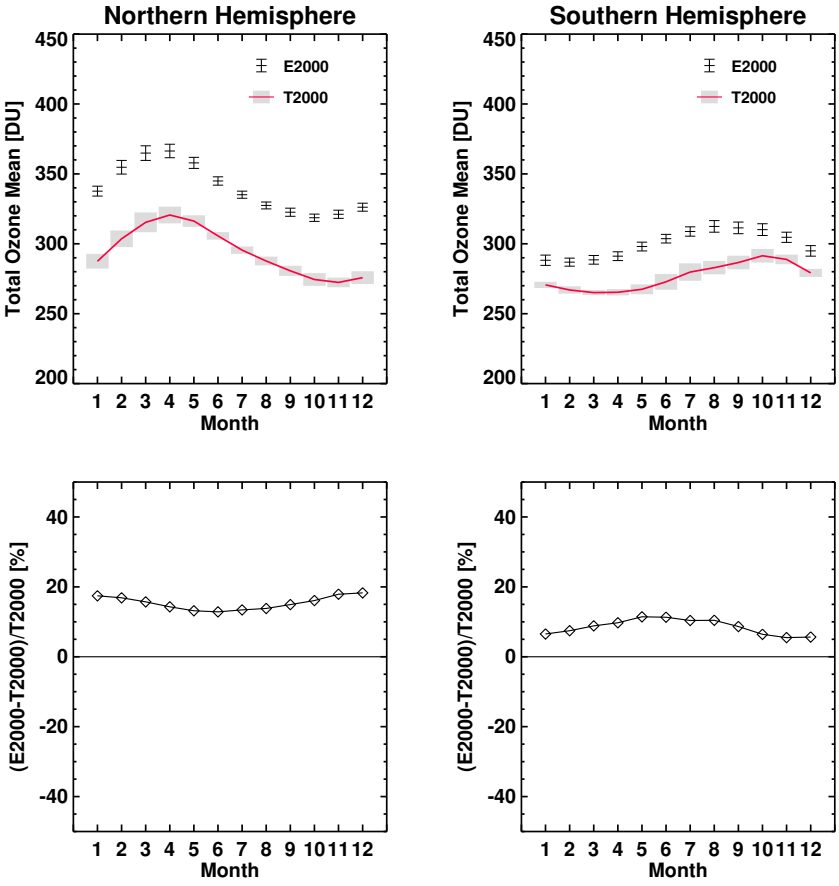

Fig. 4. Hemispheric monthly means of total ozone for E2000 and T2000 (Northern Hemisphere left, Southern Hemisphere right). Mean and standard deviation for E2000 is depicted by bars in black, T2000 mean by a solid (red) line with grey bars indicating the standard deviation (top). Below the corresponding relative differences are shown. Diamonds denote statistically significant differences of the population means at the 5% level (i.e. confidence interval of 95%).

Northern Hemisphere and its sequence of warm and cold winters. However, we are not aiming at a trend analysis and concentrate on evaluating the general deviations on a zonal and hemispheric scale. Although E2000 consists of 20 years the model mainly tends to underestimate the zonal standard deviation compared to T2000. Further, the peculiarity of the vortex split in austral spring 2002 does not show up as increased standard deviation or difference (September not shown here).

To give a more general picture of the model's ability to reproduce total ozone budgets and to increase statistical significance compared to zonal means the findings from above (Fig. 3) are summarized in a hemispheric diagnostic. Area weighted zonal mean values are averaged for each hemisphere. Figure 4 shows the hemispheric total ozone means for each month of E2000 and T2000 (top) as well as the corresponding relative differences (bottom). In both hemispheres the mean annual cycle is well reproduced by E39/C. However, a positive bias in E2000 is evident for both hemispheres and all months. For the Northern Hemisphere the relative difference is largest in December (18.2%) and smallest in June (12.8%). Largest differences for the Southern Hemisphere occur in May (11.4%) and smallest in November (5.5%). This agrees with the results of Hein et al. (2001) and Schnadt et al. (2002). Thus, it can be concluded that none of the model improvements described in Sect. 2.2 has reduced the positive total ozone bias. Recent studies further confirm that the bias is not related to the uppermost model level of E39/C centred at 10 hPa nor to the diffusive transport scheme. The positive bias is also evident in other models of the ECHAM model family like the middle-atmosphere version of ECHAM/CHEM (MA-ECHAM/CHEM) with a top level at 0.1 hPa and SOCOL using a less diffusive transport scheme. (Steil et al., 2003; Steinbrecht et al., 2006; Eyring et al., 2006). To this date the positive bias poses an unsolved problem that cannot be attributed to a single process or model feature.

4.2.2 Zonal amplitudes of wave one

In order to analyse the variability in E2000 and T2000, the amplitude of the zonal wave number one in total ozone is derived as a function of latitude (Fig. 5).

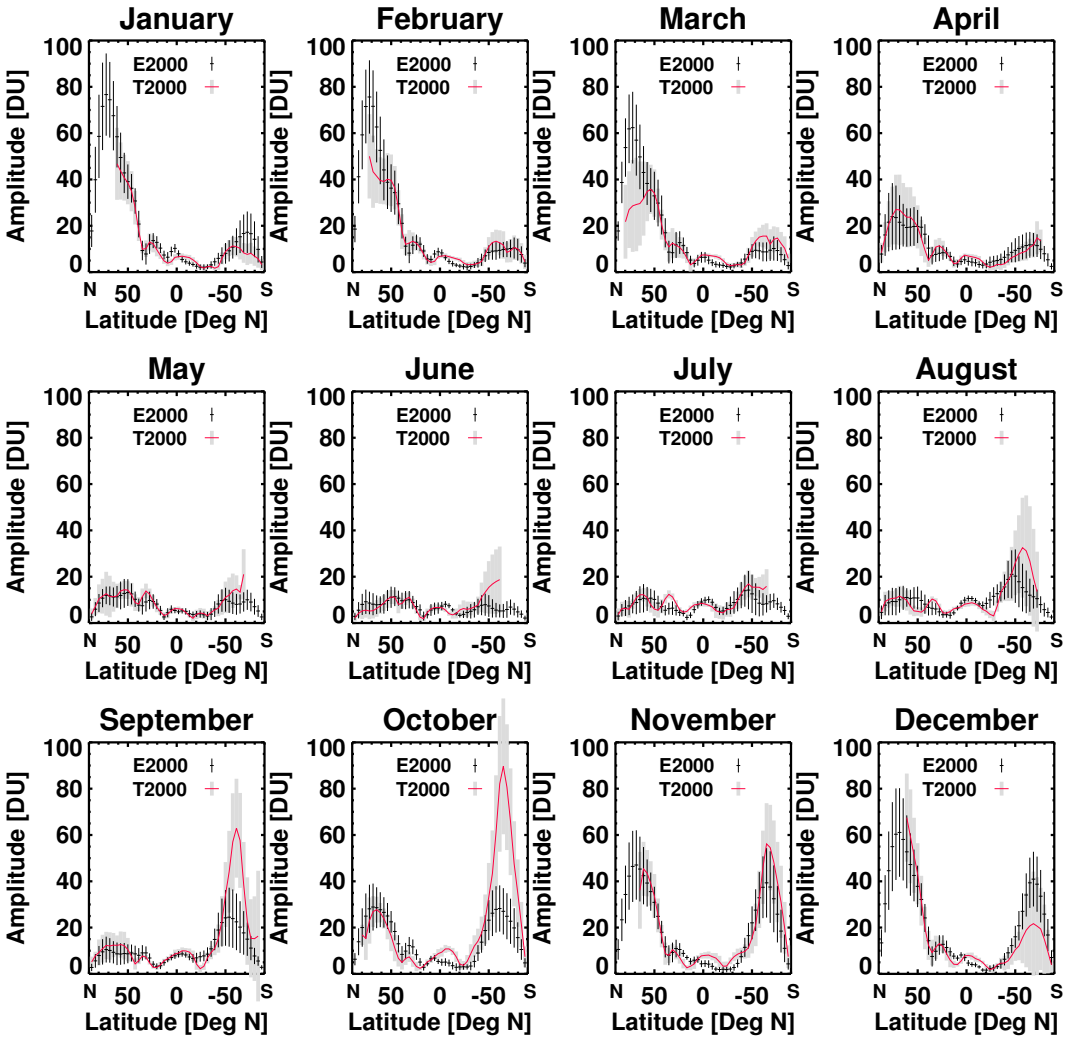

Fig. 5. Zonal amplitudes of wave number one as a function of latitude for each month for E2000 and T2000. Mean and standard deviation are indicated by black bars for E2000 and by the solid (red) curve and grey bars for T2000.

First we focus on the results for T2000 as reference. In the Northern Hemisphere high amplitudes dominate in winter and spring, low ones during summer and autumn. Maxima are found between about 60° and 70° N. In general, there is a decrease in zonal amplitude towards the tropics. Two local minima can be identified. One can be found throughout the year at 30° N–40° N, which could be associated with the subtropical transport barrier. Another pronounced minimum is detected at 10° N in winter, shifting to 20° N in summer and moving back again southwards from October on. This feature is attributed to effects related to the ITCZ. Within the minimum the amplitudes of wave one are reduced nearly to zero. This corresponds to the area of low total ozone variability in the tropics.

The variability traced by the amplitude of wave number one in the Southern Hemisphere is dominated by processes related to the polar vortex. Massive ozone depletion and offpole displacements of the polar vortex result in large amplitudes peaking in October (90 DU). The mean development of the polar vortex (and the associated Antarctic ozone hole) and its interannual variability from August to December are clearly identifiable.

A subtropical minimum can be identified at about 30° S from January to March which shifts northwards to 15° S until August and then moves back. No counterpart, however, can be identified for the second local minimum (see above).

In the following we outline the relative differences of the T2000 wave number one amplitudes with respect to E2000. When comparing E2000 to T2000 the agreement of both, mean and standard deviation, is especially strong from April to December for latitudes north of 50° N where no significant differences can be found. However, for the Northern Hemisphere large deviations can be identified in February and March north of 60° N, where E2000 exceeds T2000 up

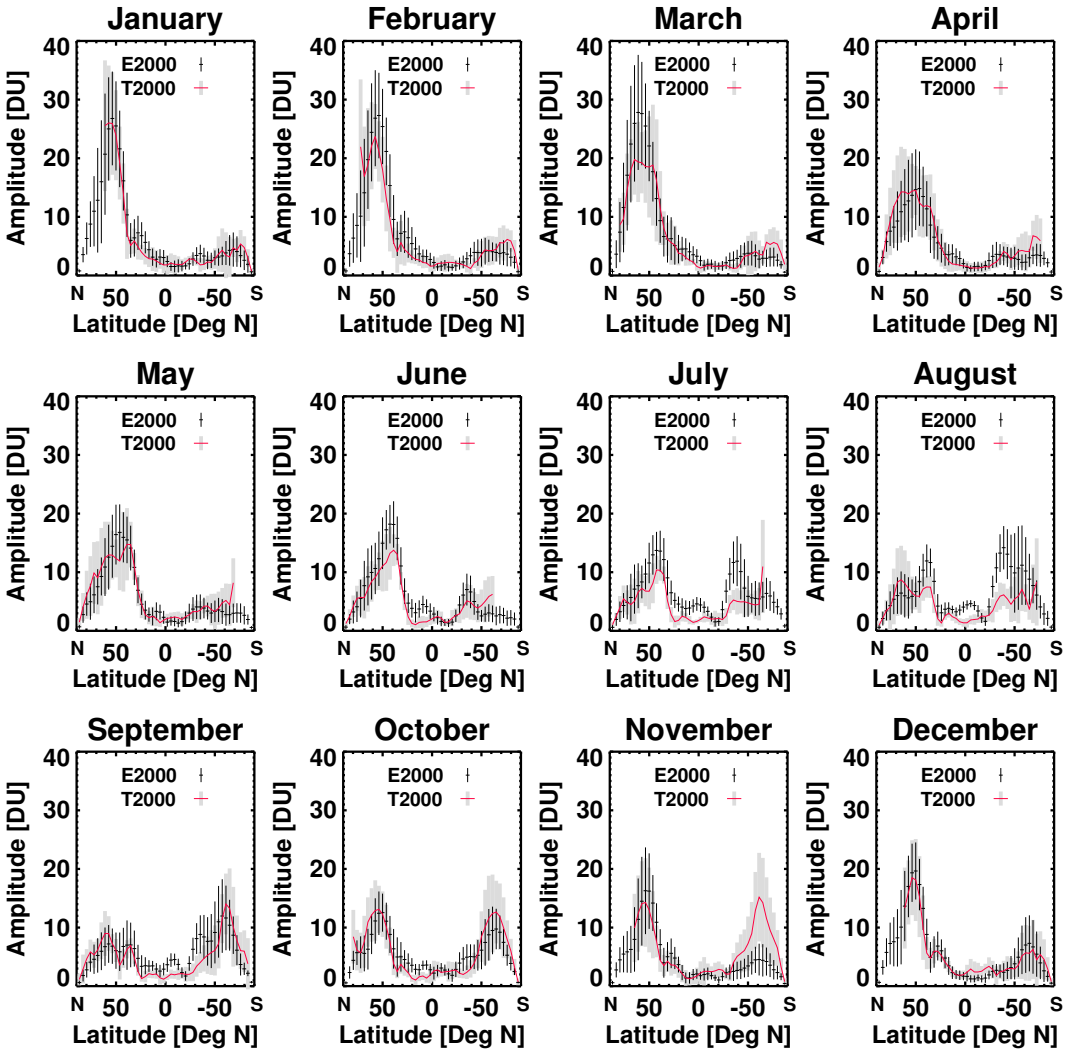

Fig. 6. Zonal amplitudes of wave number two as traced by the total ozone field as a function of latitude for each month for E2000 and T2000. Mean and standard deviation are indicated by black bars for E2000 and by the solid (red) curve and grey bars for T2000.

to 150%. Systematic deviations for a few months further occur between 40° N and 50° N. These findings reflect the problems associated with the applied semi-Lagrangian transport scheme resulting in a smoothing of gradients (Grewe et al., 2002). In particular, the transport barriers are too weak and ozone is transported (dispersed) southwards into the mid-latitudes too quickly.

However, the two local minima over the Northern Hemisphere in the tropics and subtropics already discussed above can be identified in E2000 data as well. The agreement of these smaller scale structures is good in all months except for July and August. Then, E39/C underestimates the amplitudes between 20° N and 45° N by 50% so that the local maximum at 35° N is not as pronounced as in T2000. From September to December the minima are not as pronounced as in E2000. Explicitly, the amplitudes between 10° N and 25° N are significantly overestimated in E2000 in January, February, June and October to December. It has to be emphasised, however, that small shifts of a relative maximum/minimum in meridional direction can result in large relative differences.

The most striking differences for wave one can be found during southern hemispheric spring associated with the evolution and persistence of the polar vortex. While the amplitudes south of 50° S are significantly underestimated from May to November, they are overestimated in December and January up to 120%. The comparison shows, that the modelled polar vortex and the ozone hole are too persistent, the final break down occurs about one month too late. This is in agreement with the results of Hein et al. (2001) and Schnadt et al. (2002). The reason for that can be given here: as the amplitudes of wave one are underestimated by E39/C in September and October and the wave forcing is too weak it can be followed that the interannual variability of the ozone hole is too low and that the polar vortex is too stable in terms

of off-pole displacements which would result in large zonal amplitudes in the total ozone field. Contrary to the underestimated amplitudes south of 50° S from May to November, we identify a significant overestimation at 25° S in August and September which results in a smoothing of gradients. A further new result related to Southern Hemisphere variability is that E39/C underestimates the wave one amplitude from October to December south of 50° S by 20 to 70%. The mean and interannual variability during ozone hole conditions are reasonably met and the ozone hole season in E39/C shows a time lag of approximately three weeks (Lamago et al., 2003). Taking into account this fact, the deviations of the statistical moments are expected to be smaller. This can be regarded as a general problem when comparing CCM results with observations. To demonstrate the differences associated with a temporal shift in season we show all months here.

For both data sets a similar behaviour as a function of latitude can be observed. Distinct differences, however, are evident.

4.2.3 Zonal amplitudes of wave two

Results for wave number two are shown in Fig. 6. The latitudinal distribution for each month is to some extent similar to the behaviour of the wave one amplitudes in Fig. 5 (note the different range of the ordinate). For both data sets, T2000 and E2000, small amplitudes can be found in the tropics throughout the year. Maximum values in the Northern Hemisphere of about 20 DU to 26 DU occur from January to March at 60° N. In the Southern Hemisphere maxima of 12 DU to 15 DU can be found from September to November at 60° S. Despite some exceptions, E2000 matches the statistical moments of the zonal amplitudes as function of latitude well. The latitudinal position of the maxima is met in each month. A very good agreement is obvious for the steep gradients in the amplitudes in the Northern Hemisphere between 40° and 50°, especially in January and December. From January to May model and observations fit well in the tropics and subtropics. From June to September E2000 forms a relative maximum shifting from 10° N to 10° S which is not evident in the observations.

In the Southern Hemisphere E2000 shows a pronounced relative maximum at 30° to 40° N from June to August. Since this relative maximum is not that distinct in T2000, mean and standard deviation are greatly overestimated in the model. The amplitudes are generally overestimated in the Southern Hemisphere from July to September, but are too small in October and November. In November at 65° S E2000 underestimates the amplitudes by a factor of 3.5. In December the deviation is not significant anymore. To summarize, the signature of wave number two in the total ozone fields is too weak during the ozone hole season. Especially in October and November a strong wave two contribution characterises vortex elongation and erosion, which eventually leads to the final warming.

We can infer from Figs. 5 and 6 that the conclusions are very heterogeneous and in part difficult to interpret, especially when multi-model comparisons are carried out. Therefore, we propose a hemispheric diagnostic in this study that allows a more generalised view. It reduces several zonal values to one hemispherical value. Before applying costly and specific diagnostics one can derive these indices which give a first-guess of whether the stratospheric dynamics, i.e. planetary wave activity, is represented correctly in a model.

4.2.4 Hemispheric ozone variability index 1

As already shown in Figs. 1 and 2, the hemispheric ozone variability index one shows a pronounced annual cycle for each hemisphere. Figure 7 depicts the ozone variability index one for the Northern and Southern Hemisphere derived from T2000 and E2000 respectively, and the corresponding differences (bottom). Before addressing agreements and differences, we first outline the results for T2000. Index one mirrors the annual cycles of hemispheric averaged zonal variability. In the Northern Hemisphere the observed maximum of 23 DU can be found in February, the minimum of 7 DU in June. This reflects the peaking dynamic activity in spring and the discontinued upward propagation of tropospheric waves in summer. The seasonal cycle is different in the Southern Hemisphere. The minimum of 6 DU can be found in January, the maximum of 29 DU in October. While the index ranges from 6 DU to 10 DU from January to July, we observe an increase from July to October and again a sharp decrease until December. This emphasises that the vortex displacement is clearly evident in wave number one.

We now discuss the differences in hemispheric ozone variability index one between E2000 and T2000 (Fig. 7). The findings of the detailed latitudinal analysis (Fig. 5) are well reflected and summarized in the hemispheric diagnostics. In the Northern Hemisphere strong plantery wave activity in winter and spring accompanied by ozone accumulation leads to high amplitudes of wave number one in the ozone field. The overall agreement of E2000 and T2000 is good in the Northern Hemisphere, except for the winter months. To quantify the differences, E2000 overestimates the amplitudes in wave one significantly from October to March by 21% to 55%. Beside too much activity at wave one, this could further indicate that the transition to the winter circulation is mostly too fast and the mean winter circulation itself in spring over-persistent. Concerning the interannual variability, E39/C shows too much variability in all months except for March to May. The overestimation is highest during winter.

In the Southern Hemisphere the off-pole displacement of the polar vortex and the depth of the ozone hole strongly contribute to the signal. While model and observations coincide well in amplitude and their interannual variability from January to August, despite a negative bias, they start to differ during the ozone hole season. The index one shows too small

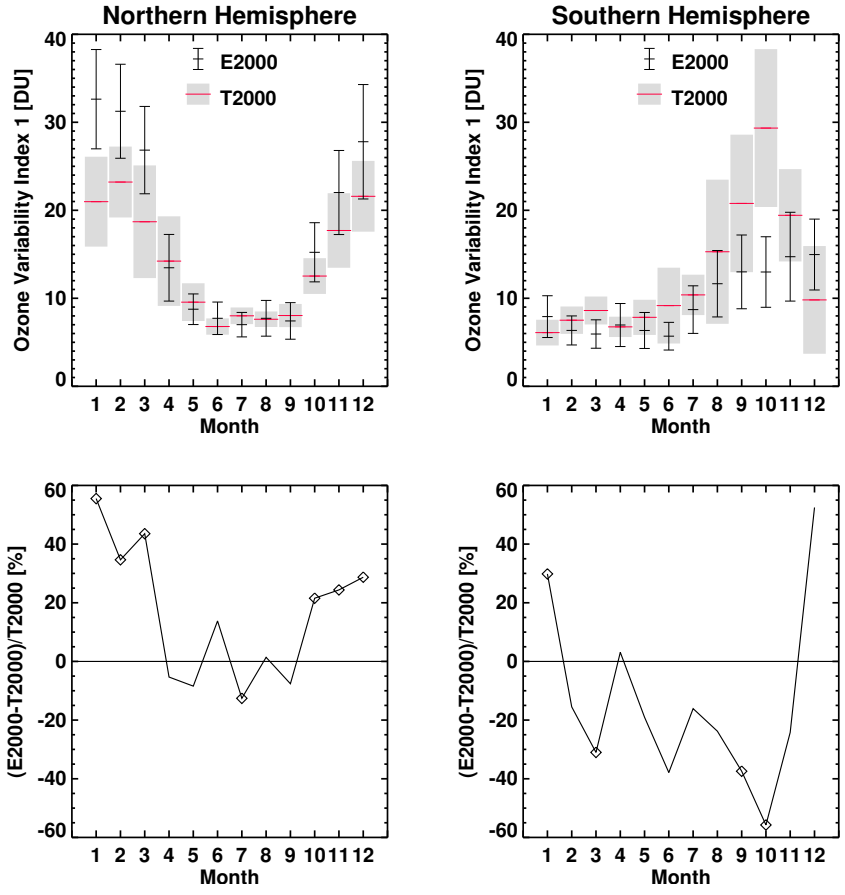

Fig. 7. Hemispheric ozone variability index 1 for each month covering the years of E2000 and T2000 (Northern Hemisphere left, Southern Hemisphere right). Mean and standard deviation are indicated by black bars for E2000 and by red dashes and grey bars for T2000 (top). Below the corresponding relative differences are depicted. The diamonds indicate statistically significant differences of both population means at the 5% level (i.e. confidence interval of 95%).

values by the model during ozone hole season in September (–38%), October (–56%) and November (–25%). The interannual variability of the ozone hole concerning off-pole displacement and depth is underestimated by E2000. An overestimation of the index one in December and January by 52% and 30%, respectively, indicates again the too persistent ozone hole in the model. Thus, also the interannual variability for January is slightly overestimated by E39/C.

4.2.5 Hemispheric ozone variability index 2

The T2000 values of index two were already discussed in Fig. 2 (bottom) for all TOMS Version 8 observations from 1978 to 2004. For comparison with E2000 the following observations are confined to the period 1996 to 2004 (Fig. 8). Nevertheless, the statistical moments for wave two and their annual cycle are similar for both periods. Since trend analysis is not a subject of this study the differences are not discussed taking into account significance.

As can be inferred from T2000, the annual cycle of the hemispheric ozone variability index two for the Northern Hemisphere shows the maximum of 11 DU in January and the minimum of 4.5 DU occurring in September. In the Southern Hemisphere the index shows a relatively smooth behaviour with an annual amplitude range of 3 DU only. A weak increase from January (3 DU) to November (6 DU) can be detected, followed by a decrease in December to 3.5 DU. When comparing T2000 with respect to E2000 we find for the Northern Hemisphere a significant overestimation of up to 44% in the summer (June to August). For the rest of the year E39/C performs quite well. Even the year-to-year variability is matched from October to December.

For the Southern Hemisphere the picture is different. The deviations are contrary to those for the hemispheric ozone variability index one. Concerning index two we find an overestimation from July to September, peaking in 61% in August, and an underestimation of 55% in November.

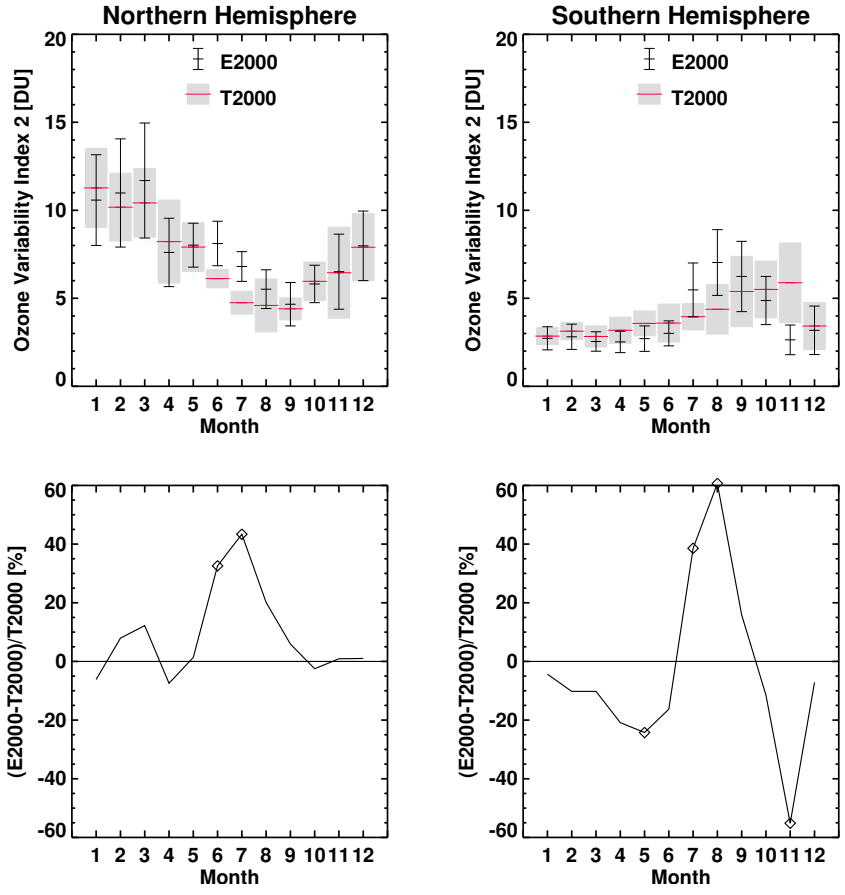

Fig. 8. Hemispheric ozone variability index 2 for each month covering the years E2000 and T2000 (Northern Hemisphere left, Southern Hemisphere right). Mean and standard deviation are indicated by black bars for E2000 and by red dashes and grey bars for T2000 (top). Below the corresponding relative differences are denoted. Diamonds indicate statistically significant differences of the population means at the 5% level (i.e. confidence interval of 95%).

5 Discussion and conclusion

In this study total column ozone observations from TOMS have been utilised to quantify the planetary wave activity in the lower and middle stratosphere. A Harmonic Analysis has been applied to derive amplitudes and phases of the planetary wave numbers one and two. Since total ozone has proven to be a valuable dynamical tracer we have presented an integrated hemispheric measure for dynamic activity.

Meeting the demand for an approach that contributes to evaluating stratospheric dynamics in CCMs, we propose the hemispheric ozone variability indices as a well suited diagnostic. It aims at analysing the representation of planetary wave activity in CCM results compared to satellite observations. It is based on a simple quantity directly derived from observed total ozone data that features proven accuracy by rigorous validation. Contrary to reanalysed meteorological data it is not influenced by model biases. Furthermore, TOMS data is easily available. The diagnostic reduces three-dimensional atmospheric quantities to an index.

In this paper the diagnostic has been exemplified with results of E39/C. Total ozone results from TOMS (T2000) have been compared to a time slice experiment (E2000).

We conclude that the hemispheric ozone variability indices one and two of E39/C are too high in the Northern and too low in the Southern Hemisphere. That means that in the model the planetary wave numbers one and two show too much activity in the Northern and too little activity in the Southern Hemisphere.

The overall agreement of both indices is better in the Northern Hemisphere. However, we have identified a strong overestimation of index one for the winter months in E39/C. Additionally, the interannual variability of index one is too strong in all months except for spring. We infer that in the Northern Hemisphere E39/C produces too strong a planetary wave one activity in winter and spring accompanied by too strong a polar vortex. Comparing mean and standard deviation of index two for all months we find for the Northern Hemisphere a significant overestimation of up to 44% in the summer. For the remainder of the year E39/C performs well.

For the Southern Hemisphere we conclude that model and observations differ significantly during the ozone hole season concerning wave one and two. As the amplitudes of both wave numbers are underestimated in September and October, E39/C exhibits too stable and strong a polar vortex. Consequently, this explains the insufficient interannual variability in the modelled ozone hole. The diagnostic further revealed a strong negative bias in planetary wave number one activity in the tropics and subtropics from October to December which may also contribute to the excessively zonal-symmetric polar vortex in the model. The general underestimation of both indices for the Southern Hemisphere is in agreement with the cold bias of the model (Dameris et al., 2005). On the contrary, we identify a strong overestimation of the index one in December and January, which explains the over-persistent ozone hole in the model.

Unlike index one, index two shows positive deviations in the Southern Hemisphere from July to September (up to 61% in August) and negative deviations by 55% in November in E39/C. There, the lack of wave two variability in October and November leads to weak vortex elongation, erosion and eventually a delayed final warming. The excessive wave number two amplitudes in July and August might cause too much meridional heat flux and contribute to the problem that the polar vortex is formed too late in season.

Since the ozone zonal mean values for the ozone hole agree well in October we link the differences mainly to dynamics. Concerning the forcing of planetary wave one and two the representation of sea surface temperatures and ice coverage should be inspected and sensitivity studies performed. The impact of interannual variations of sea surface temperatures on stratospheric dynamics and ozone was shown by Braesicke and Pyle (2004). Additionally, the underestimation of wave one might be attributed to the underestimation of the orography of the Andes. Thus, their orographic representation should be improved and its sensitivity studied. In this context also the low spatial resolution of the model has to be mentioned.

As the diagnostic is applied for each month it further allows the modelling group to identify suspicious months on a global scale for more detailed studies: e.g. index two shows significantly excessive values in July for both hemispheres. The same is the case for index one in December.

We conclude that the simple hemispheric diagnostic with its sensitive but robust quantities gains reliable results in order to quantify model-observation differences related to planetary wave activity. It is not sensitive to outliers and is therefore also suited for trend analysis. Hence, it can be applied to evaluate results of transient CCM runs.

The diagnostic is not aimed at replacing existing diagnostics nor delivering a full diagnostic of whether a model performs perfectly or not. However, we propose it as a supplement to other diagnostics defined in Eyring et al. (2005) that allows getting a first-guess on how the dynamics is represented in a model simulation before applying costly and more specific diagnostics. Finally, we would like to emphasise the straightforwardness of the diagnostic and its suitability for multi-model comparisons.

Acknowledgements. The Ozone Processing Team of NASA is kindly acknowledged for the TOMS data. The TOMS data was obtained via the World Data Center for Remote Sensing of the Atmosphere (WDC/RSAT). We would like to thank J. Austin and one anonymous referee for the review and the valuable comments.

Edited by: G. Vaughan

References

Andrews, D. G., Holton, J. R., and Leovy, C. B.: Middle Atmosphere Dynamics, Academic Press, Inc, Orlando, USA, 1987.

Appenzeller, C., Weiss, A. K., and Staehelin, J.: North Atlantic Oscillation modulates total ozone winter trends, Geophys. Res. Lett., 27, 1134–1138, 2000.

Austin, J., Shindell, D., Beagley, S. R., Brühl, C., Dameris, M., Manzini, E., Nagashima, T., Newman, P., Pawson, S., Pitari, G., Rozanov, E., Schnadt, C., and Shepherd, T. G.: Uncertainties and assessments of chemistry-climate models of the stratosphere, Atmos. Chem. Phys., 3, 1–27, 2003, http://www.atmos-chem-phys.net/3/1/2003/.

Barnett, J. J. and Labitzke, K.: Climatological distribution of planetary waves in the middle atmosphere, Adv. Space Res., 10, 63–91, 1990.

Benkovitz, C. M., Scholtz, M. T., Pacyna, J., Tarrason, L., Dignon, J., Voldner, E. C., Spiro, P. A., Logan, J. A., and Graedel, T. E.: Global gridded inventories of anthropogenic emissions of sulphur and nitrogen, J. Geophys. Res., 101, 29 239–29 253, 1996.

Bhartia, P. K. and Wellemeyer, C.: TOMS version 8 Algorithm Theoretical Basis Document, http://toms.gsfc.nasa.gov, November 24, 2004.

Bittner, M., Offermann, D., Bugaeva, I. V., et al.: Long period/large scale oscillations of temperature during the DYANA campaign, J. Atmos. Terr. Phys., 56, 1675–1700, 1994.

Bittner, M., Dech, S., and Loyola D.: Planetary scale waves in total ozone from ERS-2 GOME, ESA SP-414, 703–706, 1997.

Bojkov, R. D. and Fioletov, V. E.: Estimating the global ozone characteristics during the last 30 years, J. Geophys. Res., 100, 16 537–16 551, 1995.

Bojkov, R. D. and Balis, D. S.: Characteristics of episodes with extremely low ozone values in the northern middle latitudes 1957–2000, Ann. Geophys. 19, 797–807, 2001.

Braesicke, P. and Pyle, J. A.: Sensitivity of dynamics and ozone to different representations of SSTs in the Unified Model, Q. J. R. Meteorol. Soc., 99, 1–9, 2004.

Charney, J. G. and Drazin, P. G.: Propagation of planetary-scale disturbances from the lower atmosphere into the upper atmosphere, J. Geophys. Res., 66, 83–109, 1961.

Dameris, M., Nodorp, D., and Sausen, R.: Correlation between tropopause height, pressure and TOMS data for the EASOE-winter 1991/1992, Beitr. Phys. Atmosph., 68, 227–232, 1995.

Dameris, M., Grewe, V., Ponater, M., Deckert, R., Eyring, V., Mager, F., Matthes, S., Schnadt, C., Stenke, A., Steil, B., Brühl, C., and Giorgetta, M. A.: Long-term changes and variability in a

transient simulation with a chemistry-climate model employing realistic forcing, Atmos. Chem. Phys., 5, 2121–2145, 2005, http://www.atmos-chem-phys.net/5/2121/2005/.

Dameris, M., Matthes, S., Deckert, R., Grewe, V., and Ponater, M.: Solar cycle effect delays onset of ozone recovery, Geophys. Res. Lett., 33, L03806, doi:10.1029/2005GL024741, 2006.

Dobson, G. M. B. and Harrison, D. N.: Measurements of the amount of ozone in the earth's atmosphere and its relation to other geophysical conditions, Proc. Roy. Soc. London, A 110, 660–693, 1926.

Eyring, V., Dameris, M., Grewe, V., Langbein, I., and Kouker, W.: Climatologies of subtropical mixing derived from 3D models, Atmos. Chem. Phys., 3, 1007–1021, 2003, http://www.atmos-chem-phys.net/3/1007/2003/.

Eyring, V., Harris, N. R. P., Rex, M., Shepherd, T. G., Fahey, D. W., Amanatidis, G. T., Austin, J., Chipperfield, M. P., Dameris, M., Forster, P. M. De F., Gettelman, A., Graf, H.-F., Nagashima, T., Newman, P. A., Pawson, S., Prather, M. J., Pyle J. A., Salawitch R. J., Santer, B. D., and Waugh, D. W.: A strategy for process-oriented validation of coupled chemistry-climate models, Bull. Am. Meteorol. Soc., 86, 1117–1133, 2005.

Eyring, V., Butchart, N., Waugh, D. W., Akiyoshi, H., Austin, J., Bekki, S., Bodeker, G. E., Boville, B. A., Brühl, C., Chipperfield, M. P., Cordero, E., Dameris, M., Deushi, M., Fioletov, V. E., Frith, S. M., Garcia, R. R., Gettelman, A., Giorgetta, M. A., Grewe, V., Jourdain, L., Kinnison, D. E., Mancini, E., Manzini, E., Marchand, M., Marsh, D. R., Nagashima, T., Newman, P. A., Nielson, J. E., Pawson, S., Pitari, G., Plummer, D. A., Rozanov, E., Schraner, M., Shepherd, T. G., Shibata, K., Stolarski, R. S., Stuthers, H., Tian, W. and Yoshiki, M.: Assessment of temperature, trace spieces and ozone in chemistry-climate model simulations of the recent past, J. Geophys. Res., accepted, 2006.

Giorgetta, M. A., Manzini, E., and Roeckner, E.: Forcing of the quasi-biennial oscillation from a broad spectrum of atmospheric waves, Geophys. Res. Lett., 29, doi:10.1029/2002GL014756, 2002.

Grewe, V., Brunner, D., Dameris, M., Grenfell, J. L., Hein, R., Shindell, D., and Staehelin, J.: Origin and variability of upper tropospheric nitrogen oxides and ozone at northern mid-latitudes, Atmos. Environ., 35, 3421–3433, 2001.

Grewe, V., Dameris, M., Fichter, C., and Sausen, R.: Impact of aircraft NOx emissions. Part 1: interactively coupled climate-chemistry simulations and sensitivities to climate-chemistry feedback, lightning and model resolution, Meteorol. Z., 11, 177–186, 2002.

Haigh, J.: The impact of solar variability on climate, Science, 272, 981–984, 1996.

Hao, W. M., Liu, M.-H., and Crutzen, P. J.: Estimates of annual and regional releases of CO and other trace gases to the atmosphere from fires in the tropics, based on the FAO statistics for the period 1975–1980, in: Fire in the Tropical Biota, Ecological Studies 84, edited by: Goldammer, J. G., Springer-Verlag, New York, USA, 440–462, 1990.

Hadjinicolaou, P., Pyle, J. A., and Harris, N. R. P.: The recent turnaround in stratospheric ozone over northern middle latitudes: A dynamical modeling perspective, Geophys. Res. Lett., 32, L12821, doi:10.1029/2005GL022476, 2005.

Hein, R., Dameris, M., Schnadt, C., Land, C., Grewe, V., Köhler, I., Ponater, M., Sausen, R., Steil, B., Landgraf, J., and Brühl, C.: Results of an interactively coupled atmospheric chemistry-general circulation model: Comparison with observations, Ann. Geophys., 19, 435–457, 2001, http://www.ann-geophys.net/19/435/2001/.

Huck, P. E., McDonald, A. J., Bodeker, G. E., and Struthers, H.: Interannual variability in Antarctic ozone depletion controlled by planetary waves and polar temperatures, Geophys. Res. Lett., 32, L13819, doi:10.1029/2005GL022943, 2005.

IPCC: Climate Change 2001, The Scientific Basis, Contribution of Working Group I to the Third Assessment Report of the Intergovernmental Panel on Climate Change, edited by: Houghton, J. T., Ding, Y., Griggs, D. J., Noguer, A., van der Linden, P. J., Dai, X., Maskell, K., and Johnson, C. A., Cambridge University Press, 2001.

IPCC/TEAP (Intergovernmental Panel on Climate Change/Technology and Economic Assessment Panel), Special report on safeguarding the ozone layer and the global climate system: Issues related to hydrofluorocarbons and perfluorocarbons, prepared by working group I and III od IPCC/TEAP, edited by: Metz, B., Jager de, D., Kuijpers, L., et al., Cambridge University Press, Cambridge, United Kingdom and New York, NY, USA, 488pp., 2005.

James, P. M.: A climatology of ozone mini-holes over the Northern Hemisphere, Int. J. Climatol., 18, 1287–1303, 1998.

Kayano, M. T.: Principal modes of total ozone on the Southern Oscillation timescale and related temperature variations, J. Geophys. Res., 102, 25 797–25 806, 1997.

Labitzke, K., Austin, J., Butchart, N., Knight, J., Takahashi, M., Nakamoto, M., Nagashima, T., Haigh, J., and Williams, V.: The global signal of the 11-year solar cycle in the stratosphere: observations and models, J. Atmos. Solar-Terr. Phys., 64, 203–210, 2002.

Lamago, D., Dameris, M., Schnadt, C., Eyring, V., and Brühl, C.: Impact of large solar zenith angles on lower stratospheric dynamical and chemical processes in a coupled chemistry-climate model, Atmos. Chem. Phys., 3, 1981–1990, 2003, http://www.atmos-chem-phys.net/3/1981/2003/.

Land, C., Feichter, J., and Sausen, R.: Impact of vertical resolution on the transport of passive tracers in the ECHAM4 model, Tellus, 54B, 344–360, 2002.

McPeters, R. D., Bhartia, P. K., Krueger, A. J., Herman, J. R., Wellemeyer, C. G., Seftor, C. J., Jaross, G., Torres, O., Moy, L., Labow, G., Byerly, W., Taylor, S. L., Swissler, T., and Cebulaet, R. P.: Earth Probe Total Ozone Mapping Spectrometer (TOMS) Data Products User's Guide, NASA Reference Publication 1998-206895, 1998.

Newchurch, M. J., Yang E.-S., Cunnold, D. M., Reinsel, G. C., Zawodny, J. M., and Russell III, J. M.: Evidence for slowdown in stratospheric ozone loss: First stage of ozone recovery, J. Geophys. Res., 108, 4507, doi:10.1029/2003JD003471, 2003.

Newman, P. A. and Schoeberl, M. R.: October Antarctic Temperature and Total Ozone Trends from 1979–1985, Geophys. Res. Lett., 13, 1206–1209, 1986.

Nikulin, G. N. and Repinskaya, R. P.: Modulation of total ozone anomalies in the midlatitude Northern Hemisphere by the arctic oscillation, Izvestiya, Atm. Oceanic Phys., 37(5), 633–643, 2001.

Ortega, J. and Rheinboldt, W.: Iterative solution of nonlinear equations in several variables, New York, Academic Press, 1970.

Rayner, N. A., Parker, D. E., Horton, E. B., Folland, C. K., Alexander, L. V., Rowell, D. P., Kent, E. C., and Kaplan, A.: Global analyses of sea surface temperatures, sea ice, and nightmarine air temperature since the late nineteenth century, J. Geophys. Res., 108, 4407, doi:10.1029/2002JD002670, 2003.

Reed, R. J.: The role of vertical motions in ozone-weather relationship, J. Meteor., 7, 263–267, 1950.

Robock, A.: Volcanic eruptions and climate, Rev. Geophys., 38, 191–219, 2000.

Salby, M. L.: Survey of planetary scale travelling waves: The state of theory and observations, Rev. Geophys. Space Phys., 22, 209–236, 1984.

Sander, S. P., Friedl, R. R., DeMore, W. B., et al.: Chemical Kinetics and Photochemical Data for Use in Stratospheric Modeling, JPL Publication 00-3, NASA Jet Propulsion Laboratory, 2000.

Schoeberl, M. R., Krueger, A. J., and Newman, P. A.: The Morphology of Antarctic Total Ozone as seen by TOMS, Geophys. Res. Lett., 13, 1217–1220, 1986.

Schoeberl, M. R. and Hartmann, D. L.: The dynamics of the stratospheric polar vortex and its relation to springtime ozone depletions, Science, 251, 46–52, 1991.

Schnadt, C. and Dameris, M.: Relationship between North Atlantic Oscillation changes and stratospheric ozone recovery in the Northern Hemisphere in a chemistry-climate model, Geophys. Res. Lett., 30, doi:10.1029/2003GL017006, 2003.

Schnadt, C., Dameris, M., Ponater, M., Hein, R., Grewe, V., and Steil, B.: Interaction of atmospheric chemistry and climate and its impact on stratospheric ozone, Clim. Dynamics, 18, 501–517, 2002.

Shapiro, M. A.: Frontogenesis and geostrophically forced secondary circulations in the vicinity of jet stream-frontal zone systems, J. Atmos. Sci., 38, 954–973, 1981.

SPARC/IOC/GAW: Assessments of Trends in the Vertical Distribution of Ozone, SPARC Report No 1, http://www.aero.jussieu.fr/~sparc/SPARCReport1/, 1998.

Steil, B., Dameris, M., Brühl, C., Crutzen, P. J., Grewe, V., Ponater, M., and Sausen, R.: Development of a Chemistry Module for CGMs: first results of a multi-year integration, Ann. Geophys., 16, 205–228, 1998, http://www.ann-geophys.net/16/205/1998/.

Steil, B., Brühl, C., Manzini, E., Crutzen, P. J., Lelieveld, J., Rasch, P. J., Roeckner, E., and Krueger, K.: A new interactive chemistry-climate model. 1. Present day climatology and interannual variability of the middle atmosphere using the model and 9 years of HALOE/UARS data, J. Geophys. Res., 108, doi:10.1029/2002JD002971, 2003.

Steinbrecht, W., Hassler, B., Claude, H., Winkler, P., and Stolarski, R. S.: Global distribution of total ozone and lower stratospheric temperature variations, Atmos. Chem. Phys., 3, 1421–1438, 2003, http://www.atmos-chem-phys.net/3/1421/2003/.

Steinbrecht, W., Claude, H., and Winkler, P.: Enhanced upper stratospheric ozone: Sign of recovery or solar cycle effect?, J. Geophys. Res., 109, doi:10.1029/2003JD004284, 2004.

Steinbrecht, W. , Haßler, B., Brühl, C., Dameris, M., Giorgetta, M. A., Grewe, V., Manzini, E., Matthes, S., Schnadt, C., Steil, B., and Winkler, P.: Interannual variation patterns of total ozone and lower stratospheric temperature in observations and model simulations, Atmos. Chem. Phys., 6, 349–374, 2006, http://www.atmos-chem-phys.net/6/349/2006/.

Stolarski, R. S., Krueger, A. J., Schoeberl, M. R., McPeters, R. D., Newman, P. A., and Alpart, J. C.: NIMBUS 7 SBUV/TOMS measurements of the springtime Antarctic ozone hole, Nature, 322, 808–814, 1986.

Thomas, W., Baier, F., Erbertseder, T., and Kästner, M.: The Algeria severe weather event of November 1999 and its impact on ozone and NO2 distributions, Tellus B, 55(5), 993–1006, 2003.

Wirth, V.: Quasi-stationary planetary waves in total ozone and their correlation with lower stratosphere temperature, J. Geophys. Res., 98, 8873–8882, 1993.

World Meteorological Organisation: Scientific Assessment of Ozone Depletion: 1998 Global Ozone Research and Monitoring, Report No 44, Geneva, 1999.

World Meteorological Organisation: Scientific Assessment of Ozone Depletion: 2002 Global Research and Monitoring Project, Report No 47, Geneva, 2003.

Yang, E.-S., Cunnold, D. M., Newchurch, M. J., and Salawitch, R. J.: Change in ozone trends at southern high latitudes, Geophys. Res. Lett., 32, L12812, doi:10.1029/2004GL022296, 2005.

Yienger, J. J. and Levy II, H.: Empirical model of global soil-biogenic NOx emissions, J. Geophys. Res., 100, 11 447–11 464, 1995.

Zerefos, C. S., Bais, A., Ziomas, I. C., and Bojkov, B. R.: One the relative importance of Quasi-Biennial Oscillation and El Nino Southern Oscillation in the revised Dobson Total Ozone records, J. Geophys. Res., 100, 10 135–10 144, 1992.

Zerefos, C. S., Tourpali, K., Bojkov, B. R., Balis, D., Rognerund, B., and Isaksen, I. S. A.: Solar activity – total column ozone relationships: observations and model studies with heterogeneous chemistry, J. Geophys. Res., 102, 1561–1569, 1997.